Impact of a Patient-Derived Hepatitis C Viral RNA Genome with a Mutated MicroRNA Binding Site

Miguel Mata[1], Steven Neben[2] , Karim Majzoub[1,3], Jan Carette[1] and Peter Sarnow[1*]

1 Department of Microbiology & Immunology, Stanford University School of Medicine, Stanford, CA 94305 USA, **2** Regulus Therapeutics, San Diego, CA 92121 USA **3** INSERM U1110, Institute of Viral and Liver Disease, University of Strasbourg, 67000, France

[*]Corresponding author:
Peter Sarnow
Dept. of Microbiology & Immunology
Stanford University School of Medicine
Stanford, CA 94305
psarnow@stanford.edu

Short title: miR-122 independent growth of HCV C3U mutant

Abstract

Hepatitis C virus (HCV) depends on liver-specific microRNA miR-122 for efficient viral RNA amplification in liver cells. This microRNA interacts with two different conserved sites at the very 5' end of the viral RNA, enhancing miR-122 stability and promoting replication of the viral RNA. Treatment of HCV patients with oligonucleotides that sequester mir-122 resulted in profound loss of viral RNA in phase II clinical trials. However, some patients accumulated in their sera a viral RNA genome that contained a single cytidine to uridine mutation at the third nucleotide from the 5' genomic end. It is shown here that this C3U variant indeed displayed higher rates of replication than that of wild-type HCV when miR-122 abundance is low in liver cells. However, when miR-122 abundance is high, binding of miR-122 to site 1, most proximal to the 5' end in the C3U variant RNA, is impaired without disrupting the binding of miR-122 to site 2. As a result, C3U RNA displays a much lower rate of replication than wild-type mRNA when miR-122 abundance is high in the liver. These findings suggest that sequestration of miR-122 leads to a resistance-associated mutation that has only been observed in treated patients so far, and raises the question about the function of the C3U variant in the peripheral blood.

Author Summary

With the advent of potent direct-acting antivirals (DAA), hepatitis C virus (HCV) can now be eliminated from the majority of patients, using multidrug therapy with DAAs. However, such DAAs are not available for the treatment of most RNA virus infections. The main problem is the high error rate by which RNA-dependent RNA polymerases copy viral RNA genomes, allowing the selection of mutations that are resistant to DAAs. Thus, targeting host-encoded functions that are essential for growth of the virus but not for the host cell offer promising, novel approaches. HCV needs host-encoded microRNA miR-122 for its viral RNA replication in the liver, and depletion of miR-122 in HCV patients results in loss of viral RNA. This study shows

50 that a single-nucleotide mutation in HCV allows viral RNA amplification when miR-122
51 abundances are low, concomitant with changes in its tropism.
52
53 **Introduction**
54
55 Many cell- and virus-encoded microRNAs (miRNAs) regulate the expression of mRNAs by
56 binding to the 3' noncoding regions of target mRNAs. The binding is facilitated by an RNA-
57 induced silencing complex (RISC) that mediates base-pair interactions between nucleotides two
58 through seven in the microRNA (seed sequences) and their complementary sites in the target
59 mRNA (seed-match sequences). This targeting event inhibits the translation of the mRNA. In
60 addition, deadenylation at the 3' of the mRNA, followed by decapping and 5' to 3' degradation of
61 the mRNA greatly increases its turnover [1, 2].
62 The growth of hepatitis C virus (HCV), a member of the flaviviridae, is dependent on the
63 most abundant miRNA in the liver, miR-122 [3]. In the liver, miR-122 is known to be crucial for
64 upregulation of cholesterol metabolism [4, 5]. In the HCV genome, we discovered two binding
65 sites for miR-122 at the 5' proximal end of the viral RNA [3]. Occupancy of both sites by miR-
66 122 is required for the maintenance of viral RNA abundance in infected liver cells [3, 6-8]. Loss
67 of HCV RNA abundance could be observed when HCV-infected cells were treated with modified
68 oligonucleotides that have base-pair complementarity to miR-122 (miR-122 anti-miRs) [3]. HCV
69 sequences termed site 1 and site 2 (Fig 6A) are seed-match sequences for miR-122 and are
70 both absolutely conserved among all genotypes of HCV and present in all HCV gene sequences
71 from patients deposited in gene banks. Deleterious effects of mutations in either miR-122
72 binding site 1 or site 2 on HCV RNA accumulation can be rescued by co-transfection of mimetic
73 miR-122 duplexes that targeted the mutated HCV genomes [3, 6] [7]. Thus, HCV subverts host
74 miR-122 to increase its expression in liver cells. It is envisaged that HCV RNA genomes have
75 evolved to bind the highly abundant liver-specific miR-122 [9] to guarantee persistence in the

76 liver over many years. Mechanistically, miR-122 has been shown to protect the 5' ppp-
77 containing HCV genome from the action of 5' RNA triphosphatase DUSP11 [10, 11] and
78 subsequent degradation by 5' RNA exonucleases XRN1 [12] and XRN2 [13]. Further evidence
79 suggests that miR-122 also participates in the switch of viral RNAs from the translation to the
80 replication phase in the viral life cycle by displacing of RNA binding proteins that enhance viral
81 mRNA translation [14].
82 Clinical applications of miR-122 anti-miRs first showed that sequestration of miR-122 in
83 mice [4, 5] and in non-human primates [15] lowered plasma and liver cholesterol abundance
84 without any obvious adverse effects on liver function. Subsequently, Lanford and colleagues
85 [16] tested the effects of sequestration of miR-122 after intravenous administration of
86 unformulated locked nucleic acids (LNAs)-containing miR-122 anti-miRs in HCV-infected
87 chimpanzees. Administration of LNAs caused a 500-fold reduction of viral titer in both serum
88 and liver that persisted for several weeks. Encouraged by these results, independent studies
89 evaluated the efficacy of two different miR-122 anti-miRs, miravirsen [17] and RG101 [18], in
90 patients with chronic HCV genotype 1 infections. Treated patients showed a 10-1000 fold
91 reduction in viral serum titers. While the majority of the patients cleared the infection, several
92 subjects in both studies experienced a virologic rebound several weeks after anti-miR treatment
93 [18, 19]. Sequence analysis of viral RNAs obtained from serum of several of those patients
94 revealed a resistance-associated substitution of a uridine for a cytidine nucleotide 3 (C3U) [17,
95 18]. The goal of the present study was to examine whether the C3U mutation truly confers
96 resistance to miR-122 anti-miRs and to determine the mechanism of any such escape, to
97 provide a basis for investigation whether these variants will compromise clinical treatments.
98
99
100
101

102 **Results**

103

104 **C3U HCV RNA replicates with higher efficiency than wild-type HCV RNA during miR-122**
105 **sequestration**

106 Sera from five out of six HCV patients whose viral titers rebounded following miR-122 anti-miR
107 treatment contained HCV genomes with a C3U mutation. One patient contained a C3U/C27U
108 double mutation [18]. These findings suggested that the C3U RNA variant may replicate with
109 higher efficiency than wild-type RNA in liver cells when miR-122 is sequestrated, and thus
110 represent a drug-resistant variant.

111 To test this hypothesis, in vitro-synthesized wild-type and C3U *Gaussia* luciferase-
112 expressing H77S.3/GLuc viral RNAs (Fig 1A) [20] were transfected into Huh7.5 cells that had
113 previously been treated with non-122 targeting control anti-miR-106b-LNA, anti-miR-122-LNA
114 miravirsen [19], or anti-miR-122 RG1649 (the active metabolite of RG101) [18], and HCV RNA
115 replication was monitored. Figure 1B shows that treatment of HCV RNA-transfected cells with
116 miR-106b-LNA had no effect on wild type HCV RNA translation or replication, as reflected by
117 the accumulation of luciferase encoded in the viral genome. However, wild-type HCV RNA
118 accumulation was reduced relative to C3U HCV in miR-122 anti-miR-treated cells after 24 and
119 48 hours. These findings argue that reduced abundance of miR-122 is less inhibitory to the
120 growth of C3U HCV, thus rationalizing the emergence of the C3U genome in anti-miR-treated
121 patients.

122 To determine whether the C3U mutation acts by increasing the abundance of HCV RNA
123 following miravirsen-mediated sequestration of miR-122, the accumulation of newly synthesized
124 viral RNA was measured by labeling with 5-ethynyl uridine (5-EU), an analog of uridine. Total
125 RNA was isolated and conjugated to biotin in a copper-catalyzed reaction. Newly synthesized
126 RNA was subsequently captured using magnetic streptavidin beads and quantitated by qRT-
127 PCR using HCV-specific primers. While the abundance of wild-type RNA synthesis was reduced

128 by ~80% in miravirsen-treated samples, only a 30% reduction was observed in C3U variant
129 samples following miR-122 depletion compared to control miR-106b-LNA treatment (Fig 1C).
130 To determine whether the binding of miR-122 molecules to the C3U HCV genome plays
131 any role at all in its replication, infectious RNAs were transfected into miR-122 knock-out
132 Huh7.5 cells [21] that were pre-transfected with control duplex miR-106b or native miR-122
133 duplexes. Exogenously added control duplex failed to rescue the greatly reduced abundance of
134 either wild-type or C3U RNA. Supplementation of miR-122 duplexes enhanced the amplification
135 of both wild-type and mutant viral RNAs, albeit C3U to a significantly lesser extent than wild-
136 type RNA (Fig 1D). These results argue that C3U RNA requires at least a small amount of miR-
137 122. It is known that miR-122 has different affinities to site 1 and 2 in HCV RNA [22]. Thus,
138 different affinities for miR-122 at site 1 or site 2 in both C3U and wild-type RNAs could explain
139 the observed phenotype.
140 To test this hypothesis, C3U-complementary duplex miR-122 molecules (referred to as
141 "mut-miR-122") were employed to monitor C3U RNA replication phenotypes in cells that
142 expressed no wild-type version of miR-122. Again, pre-treatment with miR-106b RNA mimetics
143 did not rescue replication of wild-type or C3U viral RNAs (Fig 1E). As was also expected,
144 supplementation of mut-miR-122 failed to efficiently support wild-type viral RNA accumulation.
145 However, supplementation of C3U with mut-miR-122 efficiently enhanced C3U RNA
146 abundance. That both wild-type and mutant miR-122 can rescue the C3U genome to some
147 extent, but neither as completely as native miR-122 rescues the wild-type genome, suggests
148 that both wild-type and mutant miR-122 might bind to the C3U genome.
149 To substantiate this finding further, miR-122 knock-out cells were pre-transfected with
150 wild-type and mut-miR-122 duplexes alone or in combination and abundances of transfected
151 infectious RNAs were monitored over time. Co-transfection of both wild-type and mut-miR-122
152 had minimal additive effect on the accumulation of wild-type HCV RNA compared to transfection
153 of wild-type miR-122 alone (Fig 1F). In sharp contrast, accumulation of the C3U variant was

154 significantly enhanced in the presence of combined wild-type and mut-miR-122 mimetics
155 compared to the presence of either alone (Fig 1F). Analysis of viral infections by Northern blot
156 analyses (Fig. 1G) revealed the same phenotypes. These data show that a single C3U
157 nucleotide substitution in the 5' noncoding region of the HCV genomic RNA, where miR-122
158 occupies binding site 1, results in increased resistance to miR-122 sequestration. Because HCV
159 RNA accumulation in a C3U background could be effectively rescued only by a combination of
160 native and mutant-miR-122 mimetics, sites 1 and 2 in C3U RNA are likely occupied by mutant
161 and wild-type miR-122, respectively, and occupancy of both is required for its optimal function.
162 This situation is not likely to be obtained under any circumstance in liver cells, leading us to
163 question whether the C3U mutation might bring about a large fitness cost to viruses that contain
164 it.
165
166 **C3U mutation in HCV RNA reduces viral fitness in cultured liver cells**
167 To investigate the impact of the C3U HCV mutation on viral fitness in liver cells when miR-122
168 abundance is normal, in vitro-synthesized wild-type and C3U H77.S3 infectious RNAs [20] were
169 electroporated into Huh7.5 liver cells [23]. At different times after electroporation, supernatants
170 were collected and extracellular HCV titers were determined by fluorescent focus forming units
171 (FFU) measurements after infection of Huh7.5 cells (Fig 2A). In contrast to wild-type virus-
172 infected cells, which reached a maximum of 10^3 FFU/ml, virus yield was ten-fold lower in cells
173 infected with C3U HCV virus (Fig 2A). Next, viral spread was examined by infecting naïve
174 Huh7.5 cells with wild-type and mutant viruses. Supernatants were collected three days post-
175 infection and quantified by FFU assays. Similarly, to the data shown in Fig. 2A, viral production
176 (Fig. 2B) and RNA accumulation (Fig. 2C) after these multiple cycles of infection were ten-fold
177 lower in C3U HCV-infected compared to wild-type HCV-infected cells. Thus, the C3U mutation
178 results in a significant reduction in mutant viral RNA and virion abundances at a step that does
179 not involve viral entry.

180

181 **C3U mutation leads to reduced viral RNA replication in liver cells**

182 To measure the effects of the C3U mutation on viral mRNA translation and RNA replication, in
183 vitro-synthesized wild-type and C3U *Gaussia* luciferase-expressing H77S.3/GLuc viral RNAs
184 (Fig. 1A) were transfected into Huh7.5 cells and luciferase activities were examined at different
185 times after transfection. Replication of the C3U viral RNA was ten-fold lower than that of wild-
186 type RNA between 48 and 72 hours after transfection (Fig 3A). Similar to the phenotype
187 observed with luciferase activities, Northern blot analysis revealed a decrease of C3U RNA
188 abundance compared to wild-type viral RNA at three days after RNA transfection (Fig 3B). Both
189 wild-type and mutant RNAs were sensitive to the HCV RNA polymerase NS5B inhibitor
190 sofosbuvir (Fig. 3B), demonstrating that authentic viral RNAs were inspected in the Northern
191 blots and that the C3U variant can be eliminated by sofosbuvir. The effect of the C3U mutation
192 was not genotype-specific, because insertion of the C3U mutation into the J6/JFH1 RLuc
193 genotype 2a infectious background also resulted in significant reduction in RNA replication (Fig
194 S1). Finally, the abundance of viral core protein was also reduced in C3U RNA-transfected cells
195 at 72 hours compared to wild-type RNA (Fig. 3C), suggesting defects in protein synthesis, RNA
196 replication or both in C3U HCV.

197 To examine in detail whether reduced translation or replication contributed to low viral
198 RNA abundances in C3U RNA-transfected cells, we studied the expression of chimeric RNAs,
199 containing GDD-to-AAG mutations in the active site of viral RNA-dependent polymerases NS5B
200 in both wild-type and C3U RNAs. Figure 3D shows that translation of the C3U variant was
201 indistinguishable from wild-type at all time points measured, arguing that the growth defect of
202 C3U HCV is predominantly at the replication step. To examine effects of the C3U mutation on
203 HCV translation by a different approach, polysomal mRNAs were analyzed from HCV RNA-
204 transfected cells after separating cell lysates in sucrose gradients. The distribution of full-length
205 HCV RNA in each individual fraction was analyzed by Northern blot analysis (Fig. S2A). HCV

206 RNA was distributed in polysomal fractions 9 through 13 in both wild-type- and C3U-transfected
207 samples (Fig S2A,B). These data suggest that the observed reduced intracellular RNA
208 abundance of C3U HCV is primarily due to a defect in RNA replication or stability.
209
210 **Effects of the C3U substitution on viral RNA stability and nascent viral RNA synthesis in**
211 **the presence of miR-122**
212 To investigate whether the significant reduction in C3U RNA abundance in the presence of miR-
213 122 is a result of diminished RNA stability, Huh7.5 cells were transfected with HCV RNA for
214 three days and subsequently treated with the nucleoside analog MK-0608 to block viral RNA
215 synthesis. Total RNA was isolated at the indicated time points following drug treatment and the
216 rate of HCV RNA decay was examined by Northern blot analysis. Data showed that wild-type
217 HCV RNA was degraded at a slightly slower rate than C3U mutant HCV RNA (Fig 4A). The
218 approximate half-life of wild-type RNA is 3.2 hours compared to 2.6 hours for the C3U variant
219 (Fig 4A-B). Although modest, the reduction in RNA stability was statistically significant (Fig 4C)
220 and could potentially impact the fitness of the C3U virus.
221 Next, the effect of the C3U mutation on the rates of HCV RNA replication were evaluated
222 by labeling cells with 5-EU three days post viral RNA transfection. Total RNA was isolated from
223 cells pulsed for four and seven hours, captured and quantified as previously described. 5-EU-
224 labeling for up to seven hours revealed a significant ~four-fold increase in the accumulation of
225 newly-synthesized wild-type RNA compared to C3U variant RNA (Fig 4D). This impaired rate of
226 RNA synthesis coupled with a modest, but significant decrease in RNA stability are likely
227 sufficient to explain the reduced fitness of the C3U variant in the liver.
228
229 **Effects of XRN1 depletion on HCV C3U RNA abundance**
230 One explanation for the reduced abundance of C3U viral RNA during low abundance of miR-
231 122 is that reduced binding of miR-122 at site 1 could render the RNA susceptible to attack by

232 5’ RNA triphosphatase DUSP11 [10] and subsequently to 5’ -3’ exonucleases. Therefore, we
233 investigated whether the low abundance of HCV C3U RNA variant of type 1a could be rescued
234 by reducing the abundance of XRN1 by siRNA-mediated gene silencing prior to HCV RNA
235 transfection. The effect of XRN1 depletion on HCV replication was assessed by luciferase
236 activity and Northern blot analyses of chimeric RNAs. Robust XRN1 depletion was observed in
237 mock- and HCV-infected samples at 72 hours after RNA transfection (Fig 5B, top panel).
238 Depletion of XRN1 significantly stimulated the abundance of both wild-type and C3U HCV RNA
239 at 48 and 72 hours after viral RNA transfection (Fig 5A). Similarly, increased accumulation of
240 wild-type and C3U mutant HCV RNA was detected by Northern blot analysis in siXRN1-treated
241 samples (Fig 5C). The effects of XRN1 depletion on wild-type HCV replication are consistent
242 with previous observations using a similar HCV cell culture system [12]. Quantification indicated
243 that wild-type and mutant viral RNA abundances significantly increased following XRN1
244 depletion by the same extent (Fig. 5D). These data suggest that both wild-type and mutant HCV
245 RNA are similarly susceptible to XRN1 attack and that the defect in C3U RNA replication is not
246 increased degradation due to lack of miR-122 binding at site 1.
247 To explore the possibility that differences in miR-122 occupancy in the C3U variant could
248 alter its susceptibility to XRN1 attack further, we tested the stability of the replication defective
249 (GDD-to-AAG) wild-type and mutant HCV RNA synthesized with and without a 5’ non-
250 methylated guanosine cap analog after transfection into Huh7.5 cells. Viral RNAs containing a
251 cap structure or a 5’ terminal ppp-N moiety in C3U HCV displayed similar stabilities to that of
252 wild-type RNA across multiple infection time points (Fig 5E). Data from both lines of
253 investigation suggest that XRN1 is unlikely to explain the observed low C3U RNA abundance in
254 cultured liver cells.
255
256 **The C3U mutation residing in miR-122 site 1 seed sequence impairs formation of**
257 **HCV:miR-122 heterotrimeric complex in vitro**

258 The interaction between the 5' noncoding region of HCV and miR-122 at sites 1 and 2 (Fig. 6A)
259 extends beyond the canonical base pairing between seed and seed-match sequences [6, 7].
260 Mutational analysis has shown that base pairing between HCV and miR-122 at nucleotides 1-4
261 produces a 3' overhang in miR-122 that shields the viral genome from subsequent
262 exoribonuclease attack [7]. Also, previous observations indicate that the 5' terminus of HCV
263 forms a stable, trimolecular complex through interactions with the miR-122 at site 1 and 2 [22].
264 Adopting Mortimer's and Doudna's electrophoretic mobility shift assays (EMSA)
265 approach [22], we investigated whether the C3U substitution disrupted the formation of the
266 HCV:miR-122 heterotrimeric complex in solution. First, to confirm that the 5' terminus of HCV
267 genotype 1a (nucleotides 1-47) directly binds and forms an oligomeric complex with miR-122,
268 wild-type HCV RNA was incubated with increasing amounts of miR-122 and the resulting
269 complexes were resolved using EMSA. Figure 6B shows that incubation of HCV RNA with
270 different molar equivalents of miR-122 resulted in the gradual formation of a heterotrimeric
271 complex that migrated more slowly than free HCV RNA (Fig. 6B, lane 0). Incubation of HCV
272 RNA with the neuron-specific miRNA, miR-124, showed no complex formation, demonstrating
273 that the interaction between HCV and miR-122 is specific. Next, we investigated effects of the
274 C3U mutation on the formation of the heterotrimeric complexes. Figure 6C shows that the C3U-
275 containing RNA required a much higher concentration of miR-122 to form any heterotrimeric
276 complex at all. To examine whether mut-miR-122 could rescue the formation of heterotrimeric
277 complexes, wild-type or C3U RNAs were incubated with mut-miR-122 and complexes resolved
278 by EMSA. Incubation of wild-type HCV RNA with mut-miR-122 resulted in diminished formation
279 of the trimeric complex (Fig. 6D). In contrast, formation of a trimolecular complex was observed
280 after incubation of C3U RNA with mut-miR-122 (Fig. 6D). These result show that mut-miR-122
281 can bind to both site 1 and 2 in C3U RNA, but only to high-affinity site 2 in wild-type RNA.
282 Binding of mut-miR-122 to its target site is mediated by its interaction with the HCV RNA that
283 extends beyond the seed-seed match interactions. To confirm that C3U RNA and miR-122

284 interact at binding site 2, the seed sequence of miRNA binding site 1 was mutated in both wild-
285 type and C3U RNAs so that only site 2 was available for binding. Both RNAs did allow the
286 formation of dimeric, but not trimeric complexes (Fig. 6E), arguing that miR-122 can bind to site
287 2 in C3U RNA independently of site 1. These data suggest that a single C3U mutation outside
288 the seed-match region of site 1 results in reduced binding of miR-122 to site 1 but allows
289 binding of miR-122 to site 2, culminating in the formation of weak, unstable trimeric complexes.
290 It is likely that these altered miR-122/viral RNA complexes contribute to the poor viral fitness of
291 the C3U variant in the presence of miR-122 at normal abundance.
292
293
294 **Discussion**
295
296 Traditional antivirals have overwhelmingly focused on targeting virus-encoded proteins that are
297 essential components of the viral life cycle using small molecule inhibitors. Due to the high
298 mutation rates of RNA-dependent viral RNA polymerases, non-lethal mutations in the viral
299 genome can result in drug-resistance phenotypes to these direct-acting antivirals. On the other
300 hand, targeting the expression or function of host cellular factors that are vital for viral growth is
301 predicted to result in a higher genetic barrier to resistance than direct-acting antivirals. The liver-
302 expressed microRNA miR-122 was recently targeted in a miRNA-based anti-HCV therapeutic
303 strategy. Pharmacological inhibition of miR-122 using modified anti-sense oligonucleotides (anti-
304 miRs) significantly lowered the viral load in the serum of HCV-infected patients [17, 18].
305 A C3U resistance-associated mutation in the miR-122 binding site 1 of the HCV 5'
306 noncoding region was observed in sera from patients that experienced virologic rebound several
307 weeks following treatment with miR-122 anti-miRs. This led us to investigate whether this single
308 C3U substitution conferred true resistance to the inhibitory effects of anti-miRs and, if so, by
309 what mechanism viral replication could occur at lowered abundance of miR-122. While patient-

310 derived virus did not grow in cultured cells, using a cell culture-adapted HCV genotype 1a
311 infectious system we found that the C3U mutation, during sequestration of miR-122, showed an
312 increased ability to replicate the C3U RNA compared to wild-type RNA. However, this came at
313 the expense of significantly diminished viral fitness in liver cells with normal abundance of miR-
314 122. Specifically, RNA stability and rates of RNA replication of the C3U RNA are impaired in
315 cells that express normal amounts of miR-122. Curiously, the C3U mutation has not been
316 observed during selection experiments in cultured cells [17, 24, 25] and no naturally occurring
317 C3U HCV genotypes have been deposited into Gene bank. Ono et al. observed a viral G28A
318 mutation that arose in the serum and peripheral blood monocytes of type 2-infected patients
319 [25], however, the C3U variant has only been observed in patient serum after several weeks in
320 anti-miR treatment, and only transiently. Whether the extrahepatic C3U genomes reflect growth
321 of the C3U variant in the liver of re-bounding patients is not known, because liver biopsies are
322 not available. However, the poor fitness of the C3U variants suggests that the C3U variant may
323 contribute little to HCV-induced liver pathogenesis. This would be similar to the situation
324 observed with sofosbuvir, i.e. during treatment of patients with this HCV polymerase inhibitor,
325 selection is observed for variants whose fitness in the absence of the drug is so low that they do
326 not persist [26]
327 What is the mechanism by which the C3U variant can replicate in the presence of low
328 amounts of miR-122? Using genetic and biochemical approaches, we discovered that miR-122
329 binds only at site 2 in the C3U RNA. Using EMSA, Mortimer and Doudna showed that miR-122
330 binds at miRNA binding site 2 with an affinity 50-fold greater than at site 1 [22], explaining the
331 continued binding of miR-122 at site 2 in C3U even when miR-122 abundance is low. Why can
332 the C3U variant accumulate in extra-hepatic cells where miR-122 abundance is very low? It is
333 possible that novel inter- or intramolecular RNA-RNA interactions lead to stabilization of the viral
334 genomic RNA that contains the C3U mutation in the absence of miR-122. Novel RNA-protein
335 interactions could also take place at the 5' end of C3U RNAs. It will be important to identify both

336 molecular interactions that aid in its persistence, and the reservoir for the C3U variant during

337 miR-122 anti-miR treatment.

338

339

340 **Materials and Methods**

341

342 **Cell culture**

343 Huh7.5 Sec14L2 and Huh7.5 ΔmiR-122 cells (generous gifts from Charles Rice, Rockefeller
344 University, New York) were maintained in DMEM supplemented with 10% FBS, 1% non-
345 essential amino acids, and 2 mM L-glutamine (Gibco).

346

347 **In-vitro synthesized RNA and transfection**

348 Plasmids H77S.3 and H77S.3/GLuc genotype 1a [20] (generous gifts from Stan Lemon,
349 University of North Carolina, North Carolina) were transcribed using the T7 MEGAscript kit
350 (Ambion), according to the manufacturer's instructions. Huh7.5 and Huh7.5 ΔmiR-122 cells,
351 plated in 12-well dishes, were transfected with 1 μg of in vitro-transcribed (IVT) H77S.3/GLuc
352 RNA using the TransIT mRNA transfection kit (Mirus Bio LLC) according to the manufacturer's
353 protocol. After 6 hours of incubation at 37°C, supernatants were removed for GLuc assay and
354 replaced with fresh media. Supernatants were subsequently collected at 24 hours intervals.
355 Supernatants were stored at -20°C before luciferase assay.

356

357 **Fluorescent focus-forming assay**

358 Infectious titers were determined by a fluorescent focus forming units (FFU) assay. Huh7.5 cells
359 ($3X10^4$) were seeded in a 48-well plate and incubated overnight. Serial dilutions of virus stock
360 were added to cells and incubated for six hours at 37°C. The diluted virus supernatant was
361 removed and replaced with fresh medium. Media in each plate were exchanged daily. At day
362 three post-infection, cells were washed once with PBS and fixed with cold methanol/acetone
363 (1:1). HCV infection was analyzed by using a mouse monoclonal antibody directed against HCV
364 core (Abcam) at 1:300 dilution in 1% fish gelatin/PBS at room temperature for two hours and an

365 AlexFluor488-conjugated goat anti-mouse antibody (Invitrogen) at 1:200 dilution at room
366 temperature for 1 hour. The fluorescent focus forming units were counted using a fluorescence
367 microscope.
368
369 **Antisense oligonucleotides**
370 Antisense miR-122 locked nucleic acid (LNA) and RG101 have been previously described [15,
371 18].
372
373 **Viral RNA quantification using a Cell-to-Ct q-RT-PCR method**
374 3,000 Huh7.5 cells were seeded in quadruplicates in a 96-well plate one day prior to infection.
375 The following day, cells were infected with wild-type and C3U virus at an MOI of 0.005. Six
376 hours post infection, media was aspirated and replaced with fresh media. Media was replaced
377 with fresh media every day. At the indicated time post-infection, cells were lysed using the
378 Power SYBR Green Cell-to-Ct kit (Ambion), and RNAs were quantified on a Bio-rad CFX
379 Connect quantitative-PCR (qPCR) machine and Ct values were normalized to internal control
380 18S ribosomal RNA expression values. The primer sequences for the HCV H77.S3 genotype
381 were: forward 5'- CCAACTGATCAACACCAACG -3' and reverse 5'-
382 AGCTGGTCAACCTCTCAGGA -3'. The primer sequences for human 18S rRNA gene were:
383 forward 5'- AGAAACGGCTACCACATCCA -3' and reverse 5'-CACCAGACTTGCCCTCCA -3'.
384
385 **Exogenous miR-122 supplementation assay**
386 Huh7.5 ΔmiR-122 cells were plated in 12-well dishes and transfected with annealed native miR-
387 122 and mut-miR-122 duplexes (50nM) alone or in combination using Dharmafect I
388 (Dharmacon) following the manufacturer's instruction. The following day, cells were transfected
389 with 1 μg H77 GLuc IVT RNA as stated above. Twenty-four hours post H77 RNA transfection,

390 cells were re-supplemented with 50nM of native or mut-miR-122. Supernatants from transfected
391 cells were collected at the indicated time points. The following oligonucleotides were used in this
392 study: native miR-122, 5'- UGGAGUGUGACAAUGGUGUUUGU-3'; mut-miR-122, 5'-
393 UGGAGUGUGACAAUAGUGUUUGU-3'; hsa-miR-106b, 5'-UAAAGUGCUGACAGUGCAGAU-
394 3'.
395
396 **Nucleoside analogue MK-0608 treatment**
397 Huh7.5 cells, plated in 60mm dishes, were transfected with 2 μg of H77 GLuc IVT RNA as
398 stated above. Three days post-transfection, media was removed and replaced with media
399 containing MK-0608 at a final concentration of 25 μM. RNA was collected at the indicated time
400 points and HCV RNA was analyzed by Northern blot analysis. RNA half-lives were calculated
401 from three independent experiments using GraphPad Prism.
402
403 **In vitro RNA capping reactions**
404 Fifty micrograms of IVT H77 WT GLuc-AAG and H77 C3U GLuc-AAG RNAs were capped using
405 the ScriptGap m7G Capping System (Cellscript C-SCC30610) according to the manufacturer's
406 protocol. RNA was extracted using the RNeasy Mini kit (QIAGEN) following the manufacturer's
407 instructions. Purified RNA was transfected into Huh7.5 cells and samples were collected at the
408 indicated time points.
409
410 **Luciferase activity assays**
411 Following RNA transfection, secreted GLuc activity was measured in 20 μl aliquots from
412 supernatants using the Luciferase Assay System (Promega), according to the manufacturer's
413 instructions. The luminescent readings were taken using Glomax 20/20 luminometer using a 10
414 second integration time.

415

416 **Generation of H77S.3 virus**

417 Virus production was done as previously described [27]

418

419 **H77S.3 and H77S.3/GLuc mutant generation**

420 Nucleotide substitutions to pH77S.3 and pH77S.3/GLuc were completed using the
421 QuickChange Site Directed Mutagenesis Kit (Agilent), according to the manufacturer's protocol.
422 For the C3U mutation, the following primers were utilized: 5'-
423 ACGACTCACTATAGCTAGCCCCCTGATGGG-3' and 5'-
424 CCCATCAGGGGGCTAGCTATAGTGAGTCGT-3'. To introduce the lethal mutation to the NS5B
425 polymerase (GDD>AAG), the following primer were used: 5'-
426 CCATGCTCGTGTGTGCCGCCGGCTTAGTCGTTATCTG-3' and 5'-
427 CAGATAACGACTAAGCCGGCGGCACACACGAGCATGG-3'.

428

429 **Small interfering RNA transfections**

430 For XRN1-mediated depletion, the following RNAs were utilized: sense 5'-
431 GAGGUGUUGUUUCGCAUUAUUdTdT-3' and antisense 5'-
432 AATAATGCGAAACAACACCTCdTdT-3'. Sense and antisense strands were combined in 1X
433 siRNA Buffer (Dharmacon) at a final concentration of 20 μM, denatured for 2 minutes at 98°C,
434 and annealed for 1 hour at 37°C. As a negative control siRNA, the following oligonucleotides
435 were used: sense 5′- GAUCAUACGUGCGAUCAGAdTdT-3' and antisense 5'-
436 UCUGAUCGCACGUAUGAUCdTdT-3'.

437 Huh7.5 cells were seeded overnight in 12 well plates. The following day, 50 nM of siRNA
438 duplexes were transfected using Dharmafect I (Dharmacon). Following overnight incubation at
439 37°C, cells were transfected with H77S.3/GLuc, supernatants were collected at the indicated

440 time points and total RNA was extracted 3 days post-transfection. Depletion of XRN1 was
441 assessed by western blot analysis.
442
443 **Western blot analysis**
444 Cells transfected for 3 days were washed with PBS once and lysed in RIPA buffer (50 mM Tris
445 (pH 8.0), 150 mM NaCl, 0.5% sodium deoxycholate, 0.1% SDS, and 1% Triton X-100) in the
446 presence of cOmplete™,EDTA-free protease inhibitor cocktail (Roche) for 30 min on ice.
447 Lysates were clarified to remove the non-soluble fraction by centrifugation at 14,000 rpm for 10
448 min at 4°C. Protein concentrations were measured by Bradford Assay and 50 μg of total protein
449 lysate was mixed with 5X protein sample buffer containing reducing agent. Samples were
450 separated on a 10% SDS-polyacrylamide gel, transferred to a PVDF membrane (Millipore), and
451 blocked with 5% non-fat milk in PBS-T. The following primary antibodies were used to probe the
452 membranes: anti-Core (C7-50) (Abcam, ab2740), anti-Actin (Sigma), and anti-XRN1 (Bethyl Lab
453 A300-443A.) Immunoblots were developed using Pierce ECL Western Blot Substrate (Thermo
454 Fisher) following the manufacturer's suggested instructions.
455
456 **RNA isolation and Northern blot analysis**
457 Total RNA was extracted using the RNeasy Mini kit (QIAGEN). For Northern blot analysis of
458 HCV and actin RNA, 10 μg of total RNA in RNA loading buffer (32% formamide, 1X MOPS-
459 EDTA-Sodium acetate (MESA, Sigma), and 4.4% formaldehyde) was denatured for 10 minutes
460 at 65°C, separated in a 1% agarose gel containing 1X MESA and 3.7% formaldehyde,
461 transferred and UV-crosslinked to a Zeta-probe membrane (Bio-Rad) overnight. The membrane
462 was blocked and hybridized using ExpressHyb hybridization buffer (Clontech) and α-^{32}P dATP-
463 RadPrime DNA labeled probes.
464

465 **Nascent HCV RNA labeling**

466 Nascent HCV RNA transcripts were quantified using the Click-iT Nascent RNA Capture Kit
467 (Thermo Fisher) following the manufacturer's instructions. Complementary DNA was
468 synthesized using Superscript III reverse transcriptase (Thermo Fisher) following the
469 manufacturer's protocol. Newly synthesized HCV transcripts were quantified using Power SYBR
470 Green PCR Master Mix (Thermo Fisher). HCV transcript abundances were determined by
471 comparisons to standard curves obtained from in vitro transcribed H77.S3 RNA. The primer
472 sequences for the HCV H77.S3 genotype were: forward 5'- CGTGTGCTGCTCAATGTCTT -3'
473 and reverse 5'- AATGGCTGTCCAGAACTTGC -3'. Newly C3U HCV synthesized RNA
474 abundances were represented as fold change relative to EU labeling of wild-type HCV RNA.

475

476 **HCV-miR-122 electrophoretic mobility shift assays (EMSA)**

477 Wild-type and mutant HCV RNA oligonucleotides corresponding to H77S.3 domain I
478 (nucleotides 1-47) were synthesized (Stanford PAN facility). HCV domain I RNA (5 μM) was
479 mixed with 100 mM HEPES (pH 7.5), 100 mM KCl, and 5mM $MgCl_2$ in a 5 μl reaction.
480 Reactions were heated to 98°C for 3 min, cooled to 35°C for 5 min, and incubated with miR-122
481 oligos in molar ratios of 0.5, 1, 2, 3, and 4 at 37°C for 30 min. For anti-miR experiments, 1 μl of
482 miR-122 antisense oligonucleotide was added to each reaction and incubated for an additional
483 10 minutes. Five μl of RNA loading dye (30% glycerol, 0.5X TBE and 6mM $MgCl_2$) was added
484 and samples were separated in a non-denaturing gel (12% 29:1 acrylamide:bisacrylamide, 0.5X
485 TBE and 6mM $MgCl_2$) at 4°C for 2.5 hours at 20 Amps. Gel was stained with SYBR Gold
486 (Invitrogen) to visualize the HCV RNA-miR-122 interactions.

487

488

489 **Statistical Analysis**

490 Statistical analyses were performed with Prism 5 (GraphPad). A two-tailed paired
491 Student's t-test was employed to assess significant differences between two groups.
492 Error bars represent standard error of the mean.
493

494 **Acknowledgements**

495 We are grateful to Karla Kirkegaard for many helpful comments. The gifts of Huh7.5
496 Sec14L2 and Huh7.5 ΔmiR-122 cells from Joseph Luna and Charles Rice (Rockefeller
497 University, NY) are gratefully acknowledged. We are indebted to Stan Lemon (University of
498 North Carolina, NC) for receiving plasmids H77S.3 and H77S.3/GLuc genotype 1a.
499
500
501
502
503
504
505
506
507
508
509
510
511
512
513
514

515 **References**

516

517

518 1. Jonas S, Izaurralde E. Towards a molecular understanding of microRNA-mediated gene
519 silencing. Nat Rev Genet. 2015;16(7):421-33. doi: 10.1038/nrg3965. PubMed PMID: 26077373.

520

521

522 2. Wilczynska A, Bushell M. The complexity of miRNA-mediated repression. Cell Death
523 Differ. 2015;22(1):22-33. doi: 10.1038/cdd.2014.112. PubMed PMID: 25190144; PubMed
524 Central PMCID: PMCPMC4262769.

525

526 3. Jopling CL, Yi M, Lancaster AM, Lemon SM, Sarnow P. Modulation of hepatitis C virus
527 RNA abundance by a liver-specific MicroRNA. Science. 2005;309(5740):1577-81. doi:
528 10.1126/science.1113329. PubMed PMID: 16141076.

529

530 4. Esau C, Davis S, Murray SF, Yu XX, Pandey SK, Pear M, et al. miR-122 regulation of
531 lipid metabolism revealed by in vivo antisense targeting. Cell Metab. 2006;3(2):87-98. doi:
532 10.1016/j.cmet.2006.01.005. PubMed PMID: 16459310.

533

534 5. Krutzfeldt J, Rajewsky N, Braich R, Rajeev KG, Tuschl T, Manoharan M, et al. Silencing
535 of microRNAs in vivo with 'antagomirs'. Nature. 2005;438(7068):685-9. doi:
536 10.1038/nature04303. PubMed PMID: 16258535.

537

538 6. Jopling CL, Schutz S, Sarnow P. Position-dependent function for a tandem microRNA
539 miR-122-binding site located in the hepatitis C virus RNA genome. Cell Host Microbe.

540 2008;4(1):77-85. doi: 10.1016/j.chom.2008.05.013. PubMed PMID: 18621012; PubMed Central
541 PMCID: PMCPMC3519368.
542
543 7. Machlin ES, Sarnow P, Sagan SM. Masking the 5' terminal nucleotides of the hepatitis C
544 virus genome by an unconventional microRNA-target RNA complex. Proc Natl Acad Sci U S A.
545 2011;108(8):3193-8. doi: 10.1073/pnas.1012464108. PubMed PMID: 21220300; PubMed
546 Central PMCID: PMCPMC3044371.
547
548 8. Jangra RK, Yi M, Lemon SM. Regulation of hepatitis C virus translation and infectious
549 virus production by the microRNA miR-122. J Virol. 2010;84(13):6615-25. Epub 2010/04/30. doi:
550 10.1128/JVI.00417-10. PubMed PMID: 20427538; PubMed Central PMCID: PMCPMC2903297.
551
552 9. Chang J, Nicolas E, Marks D, Sander C, Lerro A, Buendia MA, et al. miR-122, a
553 mammalian liver-specific microRNA, is processed from hcr mRNA and may downregulate the
554 high affinity cationic amino acid transporter CAT-1. RNA Biol. 2004;1(2):106-13. PubMed PMID:
555 17179747.
556
557 10. Kincaid RP, Lam VL, Chirayil RP, Randall G, Sullivan CS. RNA triphosphatase DUSP11
558 enables exonuclease XRN-mediated restriction of hepatitis C virus. Proc Natl Acad Sci U S A.
559 2018;115(32):8197-202. Epub 2018/07/25. doi: 10.1073/pnas.1802326115. PubMed PMID:
560 30038017; PubMed Central PMCID: PMCPMC6094126.
561
562 11. Amador-Canizares Y, Bernier A, Wilson JA, Sagan SM. miR-122 does not impact
563 recognition of the HCV genome by innate sensors of RNA but rather protects the 5' end from
564 the cellular pyrophosphatases, DOM3Z and DUSP11. Nucleic Acids Res. 2018. doi:
565 10.1093/nar/gky273. PubMed PMID: 29672716.

566 12. Li Y, Masaki T, Yamane D, McGivern DR, Lemon SM. Competing and noncompeting
567 activities of miR-122 and the 5' exonuclease Xrn1 in regulation of hepatitis C virus replication.
568 Proc Natl Acad Sci U S A. 2013;110(5):1881-6. doi: 10.1073/pnas.1213515110. PubMed PMID:
569 23248316; PubMed Central PMCID: PMCPMC3562843.
570
571 13. Sedano CD, Sarnow P. Hepatitis C virus subverts liver-specific miR-122 to protect the
572 viral genome from exoribonuclease Xrn2. Cell Host Microbe. 2014;16(2):257-64. doi:
573 10.1016/j.chom.2014.07.006. PubMed PMID: 25121753; PubMed Central PMCID:
574 PMCPMC4227615.
575
576 14. Masaki T, Arend KC, Li Y, Yamane D, McGivern DR, Kato T, et al. miR-122 stimulates
577 hepatitis C virus RNA synthesis by altering the balance of viral RNAs engaged in replication
578 versus translation. Cell Host Microbe. 2015;17(2):217-28. doi: 10.1016/j.chom.2014.12.014.
579 PubMed PMID: 25662750; PubMed Central PMCID: PMCPMC4326553.
580
581 15. Elmen J, Lindow M, Schutz S, Lawrence M, Petri A, Obad S, et al. LNA-mediated
582 microRNA silencing in non-human primates. Nature. 2008;452(7189):896-9. doi:
583 10.1038/nature06783. PubMed PMID: 18368051.
584
585 16. Lanford RE, Hildebrandt-Eriksen ES, Petri A, Persson R, Lindow M, Munk ME, et al.
586 Therapeutic silencing of microRNA-122 in primates with chronic hepatitis C virus infection.
587 Science. 2010;327(5962):198-201. doi: 10.1126/science.1178178. PubMed PMID: 19965718;
588 PubMed Central PMCID: PMC3436126.
589
590 17. Ottosen S, Parsley TB, Yang L, Zeh K, van Doorn LJ, van der Veer E, et al. In vitro
591 antiviral activity and preclinical and clinical resistance profile of miravirsen, a novel anti-hepatitis

592 C virus therapeutic targeting the human factor miR-122. Antimicrob Agents Chemother.
593 2015;59(1):599-608. doi: 10.1128/AAC.04220-14. PubMed PMID: 25385103; PubMed Central
594 PMCID: PMCPMC4291405.
595
596 18. van der Ree MH, de Vree JM, Stelma F, Willemse S, van der Valk M, Rietdijk S, et al.
597 Safety, tolerability, and antiviral effect of RG-101 in patients with chronic hepatitis C: a phase
598 1B, double-blind, randomised controlled trial. Lancet. 2017;389(10070):709-17. doi:
599 10.1016/S0140-6736(16)31715-9. PubMed PMID: 28087069.
600
601 19. Janssen HL, Reesink HW, Lawitz EJ, Zeuzem S, Rodriguez-Torres M, Patel K, et al.
602 Treatment of HCV infection by targeting microRNA. N Engl J Med. 2013;368(18):1685-94. doi:
603 10.1056/NEJMoa1209026. PubMed PMID: 23534542.
604
605 20. Shimakami T, Welsch C, Yamane D, McGivern DR, Yi M, Zeuzem S, et al. Protease
606 inhibitor-resistant hepatitis C virus mutants with reduced fitness from impaired production of
607 infectious virus. Gastroenterology. 2011;140(2):667-75. doi: 10.1053/j.gastro.2010.10.056.
608 PubMed PMID: 21056040; PubMed Central PMCID: PMCPMC3155954.
609
610 21. Luna JM, Scheel TK, Danino T, Shaw KS, Mele A, Fak JJ, et al. Hepatitis C virus RNA
611 functionally sequesters miR-122. Cell. 2015;160(6):1099-110. Epub 2015/03/15. doi:
612 10.1016/j.cell.2015.02.025. PubMed PMID: 25768906; PubMed Central PMCID:
613 PMCPMC4386883.
614
615 22. Mortimer SA, Doudna JA. Unconventional miR-122 binding stabilizes the HCV genome
616 by forming a trimolecular RNA structure. Nucleic Acids Res. 2013;41(7):4230-40. doi:
617 10.1093/nar/gkt075. PubMed PMID: 23416544; PubMed Central PMCID: PMCPMC3627571.

618 23. Saeed M, Andreo U, Chung HY, Espiritu C, Branch AD, Silva JM, et al. SEC14L2
619 enables pan-genotype HCV replication in cell culture. Nature. 2015;524(7566):471-5. doi:
620 10.1038/nature14899. PubMed PMID: 26266980; PubMed Central PMCID: PMCPMC4632207.
621
622 24. Israelow B, Mullokandov G, Agudo J, Sourisseau M, Bashir A, Maldonado AY, et al.
623 Hepatitis C virus genetics affects miR-122 requirements and response to miR-122 inhibitors.
624 Nat Commun. 2014;5:5408. doi: 10.1038/ncomms6408. PubMed PMID: 25403145; PubMed
625 Central PMCID: PMCPMC4236719.
626
627 25. Ono C, Fukuhara T, Motooka D, Nakamura S, Okuzaki D, Yamamoto S, et al.
628 Characterization of miR-122-independent propagation of HCV. PLoS Pathog.
629 2017;13(5):e1006374. Epub 2017/05/12. doi: 10.1371/journal.ppat.1006374. PubMed PMID:
630 28494029; PubMed Central PMCID: PMCPMC5441651.
631
632 26. Svarovskaia ES, Gane E, Dvory-Sobol H, Martin R, Doehle B, Hedskog C, et al. L159F
633 and V321A Sofosbuvir-Associated Hepatitis C Virus NS5B Substitutions. J Infect Dis.
634 2016;213(8):1240-7. Epub 2015/11/26. doi: 10.1093/infdis/jiv564. PubMed PMID: 26603202.
635
636 27. Yamane D, McGivern DR, Wauthier E, Yi M, Madden VJ, Welsch C, et al. Regulation of
637 the hepatitis C virus RNA replicase by endogenous lipid peroxidation. Nat Med. 2014;20(8):927-
638 35. doi: 10.1038/nm.3610. PubMed PMID: 25064127; PubMed Central PMCID:
639 PMCPMC4126843.
640

641 **Figure Legends**

642

643 **Fig 1**. **Effects of sequestration or loss of miR-122 on wild-type and C3U variant RNA**
644 **abundances and replication.**

645 (A) Top: Structure of the infectious H77.S3/GLuc construct, containing Gaussia luciferase
646 (GLuc) and foot-and-mouth disease virus 2A autoprotease 2A between the p7 and NS2
647 sequence [20]. Replication defective mutation (AAG) in the NS5B viral polymerase gene is
648 marked. (B) Effects of miR-122 sequestration using miR-106 LNA, miR-122-LNA or RG1649
649 anti-miRs. Viral RNA replication was measured by luciferase production at the indicated time
650 points. Data is presented relative to the luciferase expression of negative control miR-106b-LNA
651 treatment. (C) Rate of replication following miR-122 sequestration. Cells were treated as in (B)
652 and 24 hours post RNA transfection, RNA was labeled with 200 μM 5-ethynyl uridine (EU) for
653 twenty-four hours, conjugated to biotin and subsequently isolated with streptavidin beads. RNA
654 replication rates were determined by qRT-PCR. Data is presented as percent labeling relative to
655 of miR-106b-LNA control treated samples (**$p<0.0034$). (D-F) HCV RNA replication in ΔmiR-
656 122 Huh7 transfected cells. Cells were pretreated with miR-106b, native miR-122, mut-miR-122
657 alone or in combination one day before and one day after HCV RNA transfection. Supernatants
658 were collected at the indicated time points and GLuc activity was determined. The data are
659 representative of 3 independent replicates (**$p<0.005$, ***$p<0.001$ ****$p<0.0001$). (G) HCV and
660 actin RNA abundances, monitored by Northern blot analysis, at 72 hours post RNA transfection.

661

662

663 **Fig 2. Effects of the C3U single nucleotide substitution on HCV genotype 1a virus**
664 **production.**

665 (A) Extracellular virus production. Huh7.5 cells were electroporated with 10 μg of infectious HCV
666 genotype 1a (H77) RNA that does not (WT) or does contain the C3U mutation. Titers were
667 determined by focus forming assays (FFU). Dotted line indicates threshold of detection. (B)
668 Virus titers of Huh7.5 cells infected with wild-type and C3U H77 variants at a multiplicity of
669 infection (moi) of 0.005 and assayed at 72 hours post infection (**** $p<0.0001$). (C) RT-qPCR
670 measurement of HCV viral RNA abundance at 5 days post-virus infection at an MOI of 0.005.
671 Data normalized to internal control 18S rRNA levels (**** $p<0.0001$). Error bars display +/- SD.
672

673 **Fig 3**. **Effects of C3U mutation on HCV RNA replication and translation.**
674 (A) HCV RNA replication was monitored by the expression of GLuc secreted into the
675 supernatants of wild-type and C3U RNA transfected Huh7.5 cells. Supernatants were collected
676 at the indicated time points. (B) Wild-type and C3U H77.S3/GLuc RNA abundances three days
677 post-transfection in untreated and cells treated with the NS5B inhibitor sofosbuvir (500nM). (C)
678 Effects of C3U mutation on HCV core protein levels examined by Western blot analysis at three
679 days post-H77.S3/GLuc RNA transfection. (D) Translation of the replication defective (AAG)
680 wild-type and C3U H77.S3/GLuc RNAs at multiple several points post-transfection. The data are
681 representative of 3 independent replicates (****$p<0.0001$,Student's t-test).
682

683 **Fig 4. Viral RNA stability and rates of replication in wild-type and C3U variants in the**
684 **presence of miR-122.**
685 (A) Effect of the C3U mutation on HCV RNA decay. Huh7.5 cells were transfected with wild-type
686 and C3U H77.S3/GLuc RNA, treated with 25 μM of MK-0608 three days later, and viral RNA
687 abundances were monitored at specific times after treatment, using Northern blot analyses. (B)
688 One phase decay graph of HCV RNA (R^2 = 0.939-0.947) was determined by normalizing HCV
689 RNA levels to loading control actin from three independent experiments. Estimated half-lives

690 ($t_{1/2}$) of wild-type and C3U RNA are 3.12 hours and 2.6 hours, respectively. (C) HCV RNA half-
691 lives ($t_{1/2}$) of three independent experiments (**p<0.0018). (C) Rates of RNA replication in wild-
692 type and mutant HCV variant. Three days after HCV RNA transfection, RNA was labeled with
693 200 μM EU for 4 and 7 hours, conjugated to biotin and subsequently isolated with streptavidin
694 beads. RNA replication rates were determined by RT-qPCR and data is normalized to wild-type
695 HCV four hour labeling time point (**p<0.0047, ns = non-significant).
696
697 **Fig 5. Effect of XRN1 depletion on wildt-ype and C3U HCV RNA abundances, replication,**
698 **and viral protein expression.**
699 (A) Huh7.5 cells were transfected with non-targeting (NT) and XRN1 siRNAs one day prior and
700 twenty-four hours after transfection with wild-type and C3U H77.S3/GLuc RNAs. Viral RNA
701 replication, measured by luciferase activity in the supernatants of transfected cells, was
702 monitored for up to 72 hours (*p<0.05 and **p<0.005). (B) Efficiency of XRN1 knockdown and
703 its effects on HCV core viral protein levels were monitored by Western blot analysis three days
704 post RNA transfection. (C) Cells were treated as in (A) and HCV RNA abundances were
705 monitored by Northern blot analysis. (D) Quantification of viral RNA levels following XRN1
706 depletion normalized to actin. The data are representative of three independent replicates. (E)
707 HCV RNA stability was monitored following the addition of a 5' non-methylated guanosine cap
708 analog to wild-type and C3U replication defective viral RNAs at the indicated time points.
709
710 **Fig 6. In vitro binding assays of HCV domain I nucleotides 1-47 with native and mutant**
711 **miR-122 species.**
712 (A) Pairing interactions between two miR-122 molecules with 5' RNA sequences of HCV
713 genotype 1a (nucleotides 1-47). The position of the C3U nucleotide change is indicated. (B)
714 HCV oligonucleotides were incubated with increasing concentrations of native miR-122 or the
715 neuron-specific miR-124, and the resulting complexes were separated by native gel

716 electrophoresis mobility shift assay. The migrations of free miRNA, one miR122-HCV complex
717 (HCV:miR-122) and two miR-122-HCV complexes (HCV-miR-122^2) are indicated. (C,D) Wild-
718 type and C3U domain I RNAs were incubated with native miR-122 (C) or mutant miR-122 (D).
719 (E) The seed-match sequence of miR-122 binding site 1 in wild-type and C3U RNAs was
720 mutated and then incubated with increasing amounts of native miR-122. Resulting oligomeric
721 complexes was resolved by non-denaturing gel electrophoresis. The data are representative of
722 three independent replicates. Nucleic acids were visualized after staining with SYBR Gold
723 (Thermo Fisher).
724
725 **Supporting information captions**
726 **Figure S1. Effect of C3U mutations in J6/JHF1 viral background.** Huh7.5 cells were
727 transfected with wild-type or C3U J6/JFH1 RLuc genomes and RNA replication was determined
728 at the indicated time points.
729
730 **Figure S2. Polysomal association of C3U HCV variant.** (A) HCV RNA distribution across a
731 sucrose gradient was determined three days following transfection of Huh7.5 cells with wild-type
732 and C3U H77.S3/GLuc RNAs. Polysomal profile trace of lysates separated in 10-60% sucrose
733 gradients. Individual subunits, monosomal, and polysomal peaks are indicated (top). Detection
734 of HCV and actin RNA in sucrose fractions 2 through 13 by Northern blot analysis (middle).
735 Small (S6 rp) and large (L13a rp) ribosomal protein abundances detected by Western blot of
736 total protein isolated from input (6%) and from fractions 4 through 13 (bottom). (B) Percent of
737 HCV RNA distributed across the polysomal gradients of three independent experiments. Error
738 bars display +/- SD.
739
740 **Supplemental methods**
741

742 **Polysomal profiling**

743 Huh7.5 cells were plated at a density of $5x10^6$ one day before HCV IVT RNA transfection. The
744 following day, cells were transfected with 10 μg of HCV GLuc wild-type or C3U RNAs. Three
745 days post transfection, 100 μg/l of cycloheximide was added to each plate. Cells were incubated
746 for three minutes at 37°C, followed by wash with ice-cold PBS, and lysis directly on plate by
747 adding 600 μl of polysomal lysis buffer (20mM Tris pH 7.5, 150mM NaCl, 5mM $MgCl_2$, 1mM
748 DTT, and 100 μg/mL of cycloheximide). Lysates were incubated on ice for ten minutes with
749 periodic agitation and clarified after sedimentation at 14,000 rpm for 10 minutes at 4°C. RNA
750 abundances in the supernatants were quantified by Nano-drop and 250 μg of cleared lysates
751 were layered onto 10-60% sucrose gradients. Gradients were centrifuged at 35,000 rpm at 4°C
752 in an SW41 rotor for 165 minutes and samples were fractionated with an Isco Retriever II/UA-6
753 detector system. RNA was extracted by adding an equal volume of acid phenol/chloroform to
754 each fraction, centrifuged at 14,000 rpm for 15 minutes at 4°C. To remove any possible
755 contaminants, an equal volume of chloroform was added to the aqueous fraction and
756 centrifuged at 14,000 rpm for 10 minutes at 4°C. RNA was precipitated overnight by addition of
757 1 volume of isopropanol to the aqueous fraction and stored at 20°C. RNA was pelleted at
758 14,000 rpm for 15 minutes at 4°C, washed twice with 75% ethanol, dried for 5 minutes at room
759 temperature, and dissolved in water. HCV and actin RNA abundances across all fractions were
760 determined by Northern blot analysis. HCV RNA abundances per fraction were determined from
761 three independent experiments and quantified using ImageJ.

762

763

764

765

766

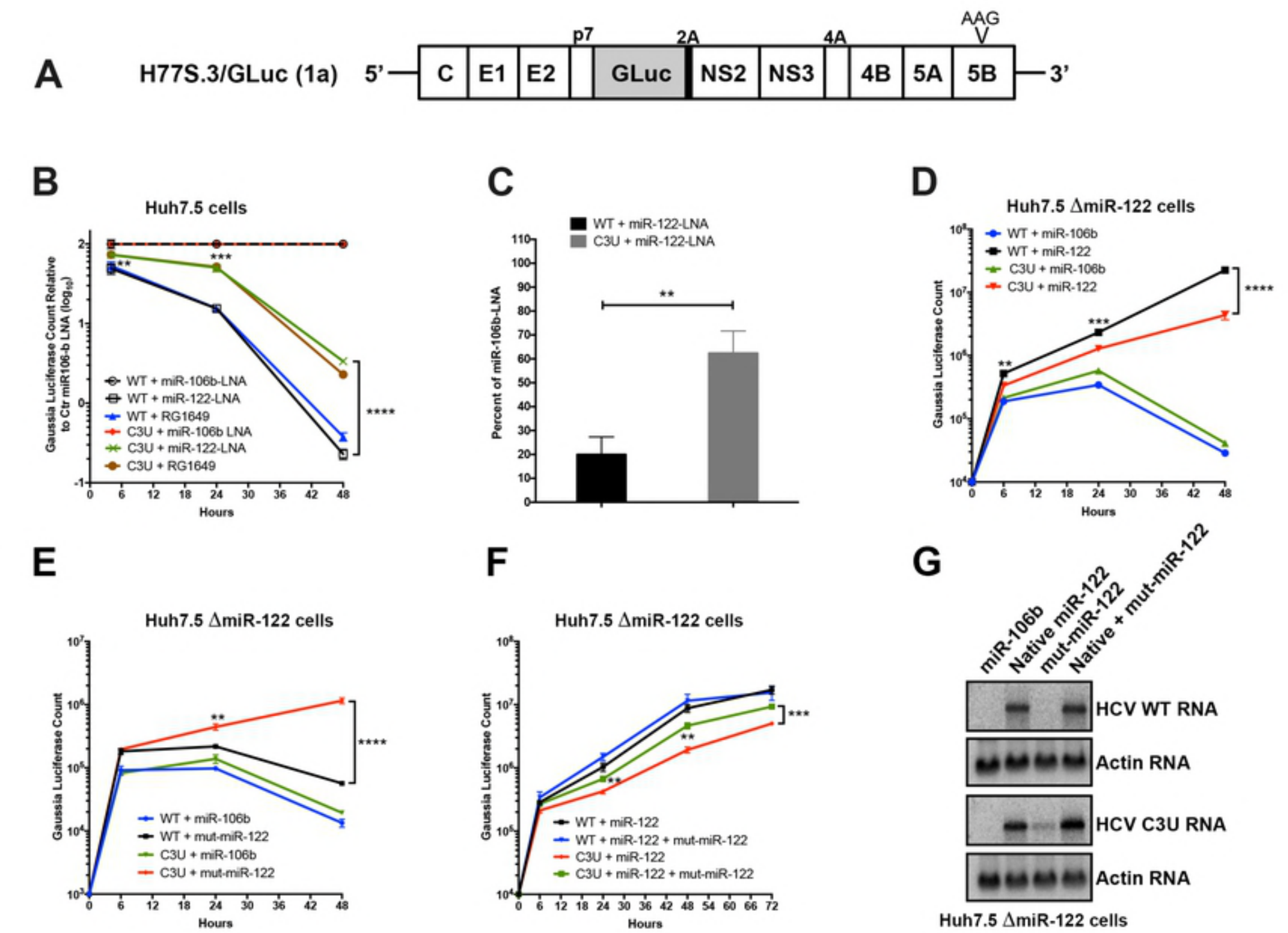
A
H77S.3/GLuc (1a)
5'
C
E1
E2
p7
GLuc
2A
NS2
NS3
4A
4B
5A
5B
AAG
V
3'
B
Huh7.5 cells
Gaussia Luciferase Count Relative to Ctr miR106-b LNA (log10)
Hours
WT + miR-106b-LNA
WT + miR-122-LNA
WT + RG1649
C3U + miR-106b LNA
C3U + miR-122-LNA
C3U + RG1649
C
WT + miR-122-LNA
C3U + miR-122-LNA
Percent of miR-106b-LNA
D
Huh7.5 ΔmiR-122 cells
Gaussia Luciferase Count
Hours
WT + miR-106b
WT + miR-122
C3U + miR-106b
C3U + miR-122
E
Huh7.5 ΔmiR-122 cells
Gaussia Luciferase Count
Hours
WT + miR-106b
WT + mut-miR-122
C3U + miR-106b
C3U + mut-miR-122
F
Huh7.5 ΔmiR-122 cells
Gaussia Luciferase Count
Hours
WT + miR-122
WT + miR-122 + mut-miR-122
C3U + miR-122
C3U + miR-122 + mut-miR-122
G
miR-106b
Native miR-122
mut-miR-122
Native + mut-miR-122
HCV WT RNA
Actin RNA
HCV C3U RNA
Actin RNA
Huh7.5 ΔmiR-122 cells

Figure